05,13

Frequency dependence of the spin mixing conductance of YIG|Pt structures upon MSSW spin pumping

© Y.V. Nikulin[1,2], S.L. Vysotskii[1,2], M.E. Seleznev[1], A.V. Kozhevnikov[1], V.K. Sakharov[1,2], G.M. Dudko[1], Y.V. Khivintsev[1,2], Y.A. Filimonov[1,2,3,¶]

[1] Saratov Branch, Kotel'nikov Institute of Radio Engineering and Electronics, Russian Academy of Sciences, Saratov, Russia
[2] Saratov National Research State University, Saratov, Russia
[3] Gagarin State Technical University of Saratov, Saratov, Russia
¶ E-mail: yuri.a.filimonov@gmail.com

Received April 17, 2023
Revised April 17, 2023
Accepted May 11, 2023

Spin pumping by traveling magnetostatic surface waves (MSSW) has been experimentally investigated in YIG|Pt structures made on the basis of 0.9, 4, 8, 14 and 18 μm thick YIG epitaxial films. It is found that at frequencies corresponding to the van Hove singularities in the density of states of the MSSW spectrum of the structure, the EMF value generated due to the inverse spin Hall effect increases. This increase is associated with an increase in the spin mixing conductance of the YIG|Pt interface due to an increase in the efficiency of electron-magnon scattering at the frequencies of van Hove singularities in the spin wave spectrum.

Keywords: spintronics, spin transport, spin waves, magnon density of states.

DOI: 10.21883/PSS.2023.06.56103.10H

1. Introduction

Layered magnetic structures based on iron yttrium garnet films ($Y_3Fe_5O_{12}$, YIG) and platinum (Pt) films are considered as one of the basic structures for developing pure spin information and communication technologies in which moving charges are replaced by dynamic objects in the form of coherent and incoherent spin waves (SW) [1–8]. Due to the exchange and spin-orbit coupling, conduction electrons in metal are bound to localized spins in a magnetic dielectric. This coupling allows, through the spin Hall effect [9,10] the conversion of electric current into a spin wave (spin current) and its further conversion into electric current (detection) using the inverse spin Hall effect [11]; detect ferromagnetic resonance [12], running spin waves [13,14], and the results of the SW interference [15]; generate coherent SW [16] and control their propagation [17].

As a parameter determining the efficiency of spin current transfer through the YIG|Pt interface, the spin mixing conductance $G^{\uparrow\downarrow}$ characterizing the difference in reflectance of the interface towards electrons with opposite spin orientations [18] is considered. The value of parameter $G^{\uparrow\downarrow}$ significantly depends on the interface quality. It has been reported that by selecting process parameters affecting the roughness, elemental composition and microstructure of the interface, the value of parameter $G^{\uparrow\downarrow}$ in YIG|Pt structures can be significantly increased [19–25].

On the other hand, parameter $G^{\uparrow\downarrow}$ reflects the efficiency of electron-magnon scattering and is determined by the density of states of both electrons and magnons [26,27]. It has previously been shown that the introduction of thin conducting layers, leading to an increase in the electron state density at the interface, is accompanied by an increase in spin conductivity $G^{\uparrow\downarrow}$ [28,29]. In the present paper, it is experimentally shown that a similar relation between parameter $G^{\uparrow\downarrow}$ and the SW density of states at the YIG|Pt interface leads to an increase in spin pumping efficiency by magnetostatic surface waves (MSSW) at van Hove [30] singularity frequencies in the SW density of states.

2. Experiment technique and examined structures

To explain the experimental procedure, we will use the standard expression for the SW density of states in the spectrum of the YIG|Pt [31] structure:

$$\eta(\omega) = \sum_k \left[e^{\beta\omega(k)} - 1 \right]^{-1}, \qquad (1)$$

where $\beta = \hbar/k_B T$, and frequency dependence $\omega(k)$ on wave number k are considered to be obtained for the chosen geometry of structure magnetization in an external magnetic field H and considering dipole, exchange, magnetoelastic interactions and magnetic anisotropy fields in the YIG film volume and when the boundary conditions for fields and magnetization are satisfied. It is very difficult to obtain an analytical expression for $\omega(k)$ when all interactions in the film are taken into account without imposing any

approximations. In dipole approximation, the character of the frequency dependence of the $\eta(\omega)$ function in the SW spectrum of a tangentially magnetized isotropic film was analyzed in [32]. It has been shown that the density of states in the MSSW spectrum experiences van Hove singularities ($\eta(\omega) \to \infty$) [30] at frequencies corresponding to the long-wave ($k \to 0$) and short-wave ($k \to \infty$) limits of the spectrum, defined, correspondingly, by expressions

$$\omega_0 = \sqrt{\omega_H^2 + \omega_H \omega_m}, \qquad \omega_s = \omega_H + \omega_m/2, \qquad (2)$$

where $\omega_H = \gamma H$, $\omega_m = \gamma 4\pi M$, γ — gyromagnetic ratio in the magnetic film, $4\pi M$ — magnetization. In the general case, it is convenient to use the frequencies ω^*, at which the group velocity of SW $v_g(\omega^*) = \partial\omega/\partial k \to 0$ [30], to find corresponding frequencies of singularities in the density of states. For MSSW, in addition to frequencies (2), frequencies ω^* may correspond to frequencies ω_n of resonant interaction of MSSW with exchange modes across the YIG film thickness [33,34], which can be written in the form

$$\omega_n = \sqrt{(\omega_H + \omega_{\text{ex}})(\omega_H + \omega_{\text{ex}} + \omega_m)}, \qquad (3)$$

where $\omega_{\text{ex}} = 2\gamma A Q^2/M$, $Q = \sqrt{k^2 + k_{\perp,n}^2}$ — total wave number, $k_{\perp,n} = \pi n/d$ — wave number across the thickness d of the film, n — mode number corresponding to the number of half-waves across the thickness, A — exchange stiffness.

Taking into account the positions of frequencies $f^* = \omega^*/(2\pi)$ in the MSSW spectrum, one can formulate requirements for the YIG films parameters and the technique of experiments with spin pumping by propagaing MSSW, at which the correlation between $\eta(\omega)$ and the spin conductivity of the YIG|Pt interface can be detected. Firstly, it is necessary to ensure that the MSSW is excited throughout the frequency band $[f_0, f_s]$, which can be realized by using microstrip antennas of width $w < d$ [31]. Secondly, it is desirable to experiment with YIG|Pt structures based on „thick“ and „thin“ YIG films, in terms of providing conditions for resonant interaction between MSSW and exchange modes [33–35]. In this case, we will consider the EMF $U(f)$ induced in Pt by the inverse spin Hall effect as a parameter characterizing the spin mixing conductivity value of the interface. It is also important to note, that the low volt-watt sensitivity of YIG|Pt structures ($S < 10^{-2}$ V/W)) forces to conduct the experiments at applied fields $H > 2\pi M = 875$ Oe, when the three-magnon processes of MSSW decay are prohibited and cannot limit MSSW power [36]. The results obtained at $H = 939$ Oe are considered in the paper.

Spin pumping by propagating MSSW in delay line (DL) type structures based on YIG|Pt films was studied experimentally, see Fig. 1. DL were fabricated using magnetron sputtering, photolithography and ion etching techniques using YIG epitaxial films of thickness $d = 0.9$, 4, 8, 14 and 18 μm. Films with $d = 8$, 14 and 18 μm were considered „thick“, while films with $d = 0.9$ and 4 μm — „thin“, as

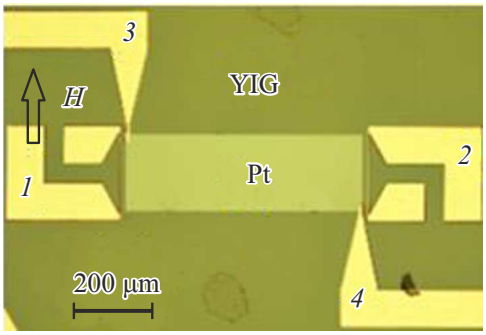

Figure 1. Photo of DL based on YIG|Pt structure. Numbers *1* and *2* denote microstrip antennas with contact pads for microprobes, *3* and *4* — contact pads to Pt film for EMF measurement.

they exhibited typical dipole-exchange resonance oscillations in MSSW transmission through DL. [34,35]. The platinum films were 8–10 nm thick, 200 μm wide and 400–800 μm long. MSSW were excited and received by copper antennas that were 250 μm long, $w = 4$ μm wide and 500 nm thick. The antennas together with the contact pads (designated *1* and *2* in Fig. 1) for the microprobe connection, as well as the *3, 4* contacts to Pt, were fabricated by lift-off lithography. Simultaneously with the DL structures, Hall bridges were manufactured which exhibited a spin Hall effect induced magnetoresistance of ~ 0.01–0.05%.

3. Results and discussion

The results shown in Fig. 2 illustrate the character of the frequency dependencies of the MSSW transmission coefficient $S_{12}(f)$, dispersion dependence $k = k(f)$ and EMF $U(f)$ for the case of structures based on „thick“ YIG films. The vertical dashed lines in Fig. 2 show the position of the long-wave $f_0 = 4.43$ GHz and short-wave $f_s = 5.09$ GHz limits of the dipole MSSW spectrum calculated with (2) at the chosen field value $H = 939$ Oe. From Fig. 2, it can be seen that the frequency interval in which the MSSW transmission and EMF generation are observed corresponds to the frequency band where Damon–Eschbach MSSW exist, and the measured dependence $k = k(f)$ almost coincides with one calculated by the formulas [32]. In the frequency dependence of EMF $U(f)$, it is possible to observe maxima near long-wave ($f_0 = 4.43$ GHz) and short-wave ($f_s = 5.09$ GHz) borders of a spectrum, Fig. 2, *c* that indicates the increase of efficiency of electron-magnon scattering on the interface at these frequencies. The dotted curve in Fig. 2, *c* shows the result of calculating the $\eta(\omega)$ dependence in the dipole MSSW spectrum of the YIG film for the $H = 939$ Oe field, carried out using the formulae [32]. It can be seen that the frequencies $f_{0,s}$, at which the EMF maxima are observed, correspond to the frequencies of singularities in the $\eta(\omega)$ density of states in the spectrum of dipole MSSWs.

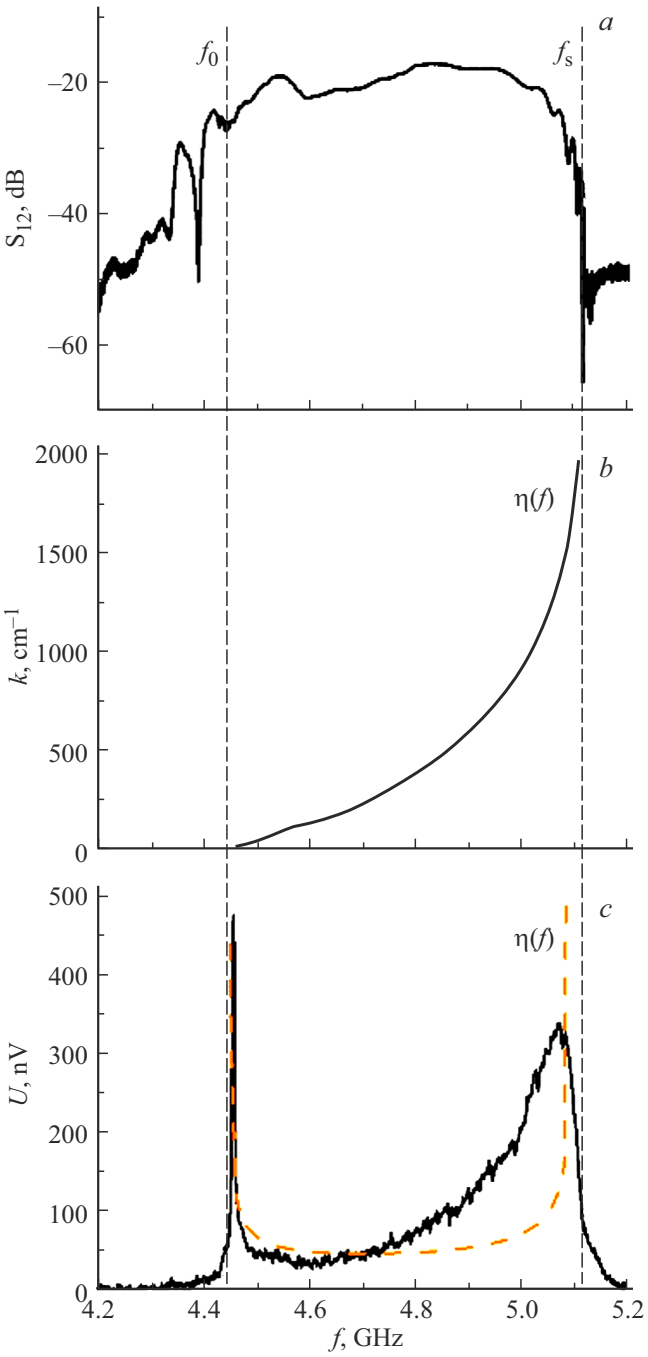

Figure 2. For YIG|Pt structure based on „thick“ film with $d = 8\,\mu$m, $H \approx 939$ Oe, the measured frequency dependencies of: *a*) transmission coefficient modulus $S_{12}(f)$; *b*) wave number of MSSW $k = k(f)$; *c*) the solid line — the generated EMF $U(f)$ at $P_{in} \approx -5$ dBm, the dashed line — the calculation by the formulas [32] for the function $\eta(f)$ of density of states in the MSSW spectrum. The vertical dashed lines show the position of the longwave (f_0) and shortwave (f_s) limits of the MSSW spectrum.

The results shown in Fig. 3 illustrate the features of propagation, EMF generation and dipole-exchange MSSW spectrum in a structure based on a „thin“ YIG film of $d = 0.9\,\mu$m thickness. Fig. 3, *a* show the frequency dependence of transmission coefficient $S_{12}(f)$ of the MSSW signal in the DL based on YIG|Pt structure and YIG film, respectively, by the curves *1* and *2*. At the frequencies highlighted by asterisks on the curve *2*, the $S_{12}(f)$ dependences show characteristic [34,35] narrow „dips“, reflecting an increase in MSSW losses due to resonance interaction with the exchange modes at frequencies (3). The curve *3* in Fig. 3, *a* shows the frequency dependence of EMF $U(f)$at incident power level $P_{in} = -5$ dBm. It can be seen that oscillations of a resonant nature are observed at the dipole-exchange frequencies in the $U(f)$ dependence. To show that the resonant EMF growth at frequencies (3) can be matched by singularities in the SW density of states, we turn to Fig. 3, *b*, which shows the results of numerical calculation of the dipole-exchange wave spectrum performed in the dissipative-free approximation within the approach [33–35]. From the insert in Fig. 3, *b*, it can be seen that at resonant frequencies, the dispersion curves of the dipole and exchange waves repulse, leading to sections of dispersion where $v_g \to 0$. With sufficiently strong SW attenuation, the repulsion of the dispersion curves disappears, an anomalous region is formed in the MSSW dispersion law, and the MSSW loss resonantly grows [34,35]. In this case, the standard approach to calculate group velocity may not be applicable due to the inability to neglect the contribution of dispersion spreading over the signal propagation time between antennas [37]. However, the very fact of a resonant growth of losses in the experiment can be interpreted as a decrease of the MSSW propagation speed, which must reflect an increase in the SW density of states $n(f)$ at frequencies f_n and be accompanied by an increase in the electron-magnon scattering efficiency.

To show that the EMF generated in the structures is due to spin current injection through the YIG|Pt interface, let us turn to Fig. 4, which shows $U(f)$ dependences for structures based on $d = 8\,\mu$m and $d = 0.9\,\mu$m films, obtained by reversing the magnetic field direction **H** and/or the MSSW propagation direction **k**. In Fig. 4, the curves *1* and *4* correspond to the applied field direction shown by the arrow in Fig. 1. The curves *1* show the dependencies for the case where the antenna *1* is taken as input and the MSSW propagates along the YIG|Pt boundary. The curves *4* show the dependencies when the antenna *2* excites the MSSW, and the wave is pressed to the boundary of the YIG film with a gadolinium gallium garnet (GGG) substrate.

The results shown in Fig. 4 with curves *2* and *3* are obtained when the structure is magnetized in the opposite direction to that shown by the arrow in Fig. 1. The curves *3*(*2*) correspond to the case, where the antenna *2*(*1*) is taken as input and the MSSW propagates along the YIG|Pt (YIG|GGG) boundary. From the results shown in Fig.4, it follows that the sign of the generated EMF is determined by the magnetic field direction, while the change of the MSSW

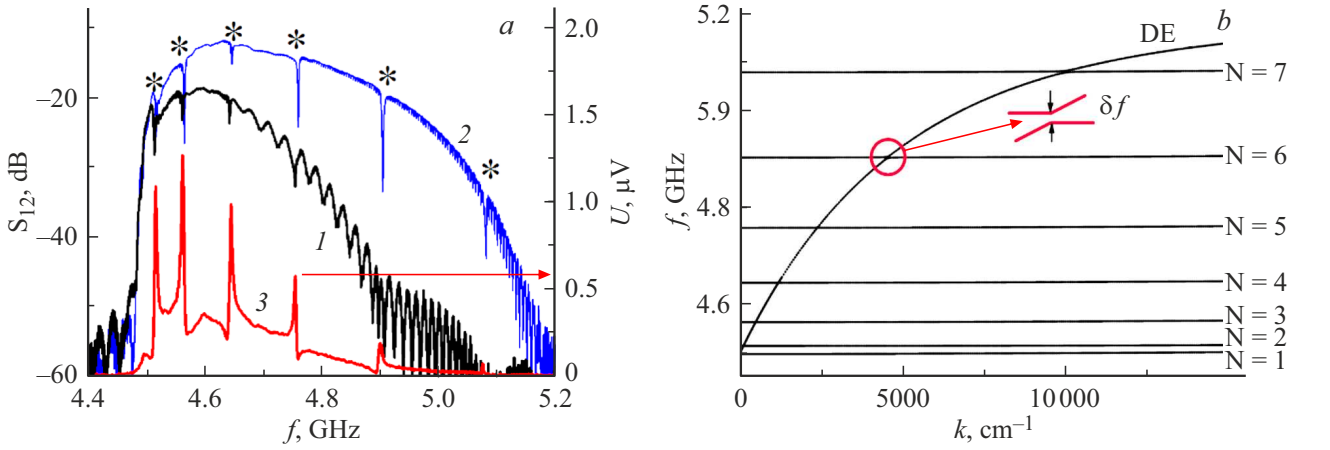

Figure 3. YIG|Pt structure based on „thin“ film with $d = 0.9\,\mu$m, $H \approx 939$ Oe. *a*) Results of the $S_{12}(f)$ transmission modulus measurements in the YIG|Pt structure (curve *1*) and YIG film (curve *2*), where asterisks indicate „dips“ due to resonant interaction of MSSW and exchange modes with number n, see Fig. 3, *b*. The curve *3* shows the frequency dependence of the generated EMF $U(f)$ at $P_{\text{in}} \approx -5$ dBm. *b*) The calculated spectrum of the dipole-exchange MSSW in an YIG film within the approach [34–36]. The number n at the horizontal curves corresponds to the exchange mode number. The figure insert illustrates the nature of the dispersion curves in the vicinity of the MSSW resonance with exchange mode with number $n = 6$ and the formation of a „gap“ $\delta f \approx 5$ MHz in the spectrum.

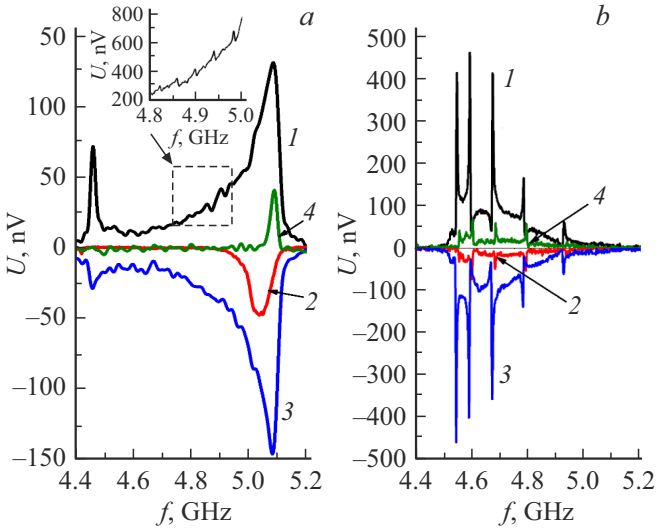

Figure 4. Dependences $U(f)$ for structures based on films with *a*) $d = 8\,\mu$m and *b*) $d = 0.9\,\mu$m, obtained by reversing the magnetic field direction **H** and/or MSSW propagation direction **k**. The curves *1, 4* and *2, 3* correspond to opposite magnetization directions. The curves *1, 3* and *2, 4* correspond to the MSSW propagation along the YIG|Pt and YIG|GGG boundaries, respectively.

propagation direction at unchanged **H** affects the signal value because of the nonreciprocal MSSW propagation.

Fig. 5 shows the frequency dependences of EMF for YIG|Pt structures based on YIG films of thickness $d = 18$, 14, 8, 4 and $0.9\,\mu$m marked by numbers *1–5* respectively. It can be seen that the frequencies at which the maxima in the dependences $U(f)$ are observed correlate with the frequencies of van Hove singularities in the density of states of the SW spectrum of the film. It should be noted that in the structure based on the film with the thickness $d = 8\,\mu$m, the frequency dependence $U(f)$ in the upper part of the range shows oscillations at frequencies of dipole-exchange resonances, see insert to the curve *1* in Fig. 4, *a*. This shows that the approach used here to divide YIG films into „thick“ and „thin“ based on the manifestation of dipole-exchange resonances in the characteristics of the propagating MSSW is not suitable for spin pumping. Indeed, increasing the thickness of the YIG film leads only to the disappearance of resonance features in the MSSW spectrum, but hybridization of the dipole MSSW with the exchange modes of the film having a low group velocity is retained and manifests, for example, in the form of radiation exchange losses of MSSW [38,39]. It is possible that the divergence in the character of the dependences of the measured EMF $U(f)$ and the calculated density of states $\eta(f)$ at frequencies near the short-wave limit of the MSSW spectrum f_s in Fig. 2 is due to this effect.

When comparing the character of the $U(f)$ and $\eta(f)$ dependences near the long-wavelength limit of the MSSW f_0 spectrum, it must be considered that magnetic anisotropy fields in the vicinity f_0 can lead to anisotropic volume magnetostatic waves (AVMSW) appearing in the film spectrum. Van Hove singularities at frequencies other than f_0 can form in the spectrum of such AVMSWs, which can noticeably affect the nature of the frequency dependence of the EMF $U(f)$ [36].

It should be noted that the spin conductivity of the YIG|Pt interface is only affected by van Hove singularities for which a high density of states in the SW spectrum is reached exactly near the interface. In the case where at

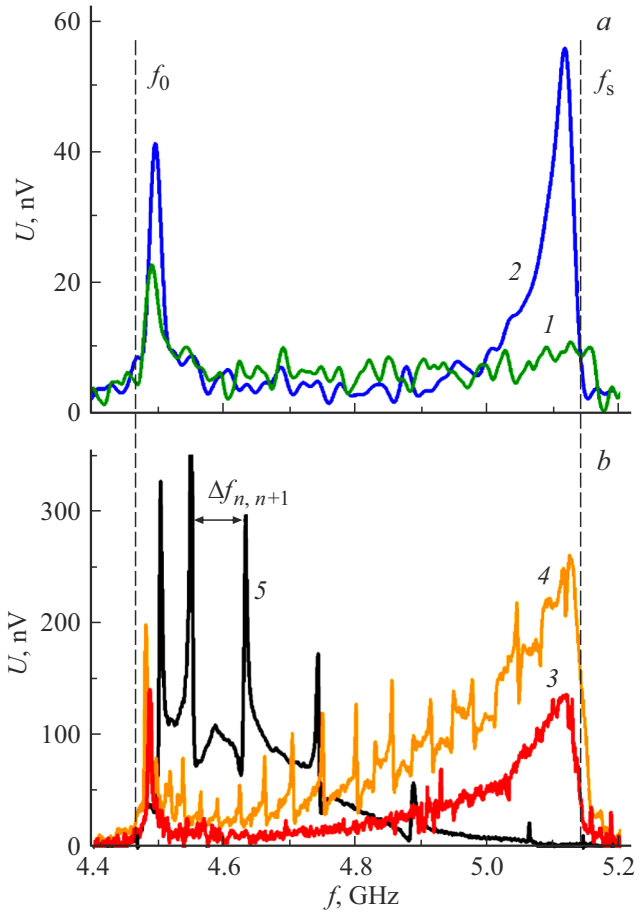

Figure 5. Frequency dependencies of EMF in YIG|Pt structures based on *a*) „thick“ and *b*) „thin“ YIG films. Numbers *1*–*5* correspond to structures based on YIG films of thickness $d = 18$, 14, 8, 4 and 0.9 μm. In curve *5* (Fig. *b*), the interval $\Delta f_{n,n+1}$ between the EMF peaks corresponds to the frequency difference for n-th and $(n+1)$-th modes of spin-wave resonance in YIG. Incident power $P = -5$ dBm. Magnetic field $H = 939$ Oe. The frequencies $f_{0,s}$ and the vertical dashed lines show the position of the long-wave and short-wave limits of the dipole MSSW [33] spectrum.

the singularity frequency in the density of states $\eta(f)$, the SWs are localized in the volume of the YIG film, their contribution to the spin conduction of the interface will be small. An example of a singularity in the density of states which does not contribute to electron-magnon scattering would be the frequency of „bottom“ $\omega_{\text{bot}} = \omega_H + \omega_{\text{ex}}$ in the spectrum of a tangentially magnetized film [36].

4. Conclusion

Thus, by the example of spin pumping by propagating magnetostatic surface waves in YIG|Pt structures, the relation of spin current transport efficiency through the interface with van Hove singularities in the density of states of the spin wave spectrum at the interface of the structure is demonstrated. The increase in spin conductivity results from an increase in electron-magnon scattering efficiency at singularity frequencies. It should be noted that at frequencies of van Hove singularities, the effective mass of magnons must increase simultaneously with the density of states, which, in turn, can also enhance the electron scattering [40].

Funding

This paper was supported by Russian Science Foundation grant No. 22-19-00500.

Conflict of interest

The authors declare that they have no conflict of interest.

References

[1] J. Sinova, S.O. Valenzuela, J. Wunderlich, C.H. Back, T. Jungwirth. Rev. Mod. Phys. **87**, *4*, 1213 (2015).
[2] A. Chumak, V. Vasyuchka, A. Serga, B. Hillebrands. Nature Phys. **11**, *6*, 453 (2015).
[3] S.A. Nikitov, D.V. Kalyabin, I.V. Lisenkov, A.N. Slavin, Yu.N. Barabanenkov, S.A. Osokin, A.V. Sadovnikov, E.N. Beginin, M.A. Morozova, Yu.P. Sharaevsky, Yu.A. Filimonov, Yu.V. Khivintsev, S.L. Vysotsky, V.K. Sakharov, E.S. Pavlov. Phys.–Usp. **58**, *10*, 1002 (2015).
[4] V.E. Demidov, S. Urazhdin, G. de Loubens, O. Klein, V. Cros, A. Anane, S.O. Demokritov. Phys. Rep. **673**, 23 (2017).
[5] M. Althammer. J. Phys. D **51**, *31*, 313001 (2018).
[6] V.E. Demidov, S. Urazhdin, A. Anane, V. Cros, S.O. Demokritov. J. Appl. Phys. **127**, *17*, 170901 (2020).
[7] A. Brataas, B. van Wees, O. Klein, G. de Loubens, M. Viret. Phys. Rep. **885**, 20 (2020).
[8] S.A. Nikitov, A.R. Safin, D.V. Kalyabin, A.V. Sadovnikov, E.N. Beginin, M.V. Logunov, M.A. Morozova, S.A. Odintsov, S.A. Osokin, A.Yu. Sharaevskaya, Yu.P. Sharaevsky, A.I. Kirilyuk. Phys.–Usp. **190**, *10*, 945 (2020).
[9] M.I. Dyakonov, V.I. Perel. Phys. Lett. A **35**, *6*, 459 (1971).
[10] J.E. Hirsch. Phys. Rev. Lett. **83**, *9*, 1834 (1999).
[11] Y. Kajiwara, K. Harii, S. Takahashi, J. Ohe, K. Uchida, M. Mizuguchi, H. Umezawa, H. Kawai, K. Ando, K. Takanashi, S. Maekawa, E. Saitoh. Nature **464**, *7286*, 262 (2010).
[12] C.W. Sandweg, Y. Kajiwara, K. Ando, E. Saitoh, B. Hillebrands. Appl. Phys. Lett. **97**, *25*, 252504 (2010).
[13] A.V. Chumak, A.A. Serga, M.B. Jungfleisch, R. Neb, D.A. Bozhko, V.S. Tiberkevich, B. Hillebrands. Appl. Phys. Lett. **100**, *8*, 082405 (2012).
[14] M. Balinsky, M. Ranjbar, M. Haidar, P. Dürrenfeld, S. Khartsev, A. Slavin, J. Åkerman, R.K. Dumas. IEEE Magn. Lett. **6**, 3000604 (2015).
[15] M. Balinskiy, H. Chiang, D. Gutierrez, A. Khitun. Appl. Phys. Lett. **118**, *24*, 242402 (2021).
[16] M. Collet, X. de Milly, O. d'Allivy Kelly, V.V. Naletov, R. Bernard, P. Bortolotti, J. Ben Youssef, V.E. Demidov, S.O. Demokritov, J.L. Prieto, M. Muñoz, V. Cros, A. Anane, G. de Loubens, O. Klein. Nature Commun **7**, 10377 (2016).

[17] M. Evelt, V.E. Demidov, V. Bessonov, S.O. Demokritov, J.L. Prieto, M. Muñoz, J. Ben Youssef, V.V. Naletov, G. de Loubens, O. Klein, M. Collet, K. Garcia-Hernandez, P. Bortolotti, V. Cros, A. Anane. Appl. Phys. Lett. **108**, *17*, 172406 (2016).
[18] Y. Tserkovnyak, A. Brataas, G.E.W. Bauer. Phys. Rev. Lett. **88**, *11*, 117601 (2002).
[19] Z. Qiu, K. Ando, K. Uchida, Y. Kajiwara, R. Takahashi, H. Nakayama, T. An, Y. Fujikawa, E. Saitoh. Appl. Phys. Lett. **103**, *9*, 092404 (2013).
[20] Y. Saiga, K. Mizunuma, Y. Kono, J.C. Ryu, H. Ono, M. Kohda, E. Okuno. Appl. Phys. Express **7**, *9*, 093001 (2014).
[21] L. Liu, Y. Li, Y. Liu, T. Feng, J. Xu, X.R. Wang, D. Wu, P. Gao, J. Li. Phys. Rev. B **102**, *1*, 014411 (2020).
[22] D. Song, L. Ma, S. Zhou, J. Zhu. Appl. Phys. Lett. **107**, *4*, 042401 (2015).
[23] M.B. Jungfleisch, V. Lauer, R. Neb, A.V. Chumak, B. Hillebrands. Appl. Phys. Lett. **103**, *2*, 022411 (2013). https://doi.org/10.1063/1.4813315
[24] Y. Sun, H. Chang, M. Kabatek, Y.-Y. Song, Z. Wang, M. Jantz, W. Schneider, M. Wu, E. Montoya, B. Kardasz, B. Heinrich, S.G.E. Te Velthuis, H. Schultheiss, A.F. Hoffmann. Phys. Rev. Lett. **111**, *10*, 106601 (2013).
[25] A. Aqeel, I.J. Vera-Marun, B.J. van Wees, T.T.M. Palstra. J. Appl. Phys. **116**, *15*, 153705 (2014).
[26] S. Takahashi, E. Saitoh, S. Maekawa. J. Phys.: Conf. Ser. **200**, 062030 (2010).
[27] E.G. Tveten, A. Brataas, Y. Tserkovnyak. Phys. Rev. B **92**, *18*, 180412 (2015).
[28] G. Li, H. Jin, Y. Wei, J. Wang. Phys. Rev. B **106**, *20*, 205303 (2022).
[29] V. Kalappattil, R. Geng, R. Das, M. Pham, H. Luong, T. Nguyen, A. Popescu, L.M. Woods, M. Kläui, H. Srikanth, M.H. Phan. Mater. Horiz. **7**, *5*, 1413 (2020).
[30] L. Van Hove. Phys. Rev. **89**, *6*, 1189 (1953).
[31] A.G. Gurevich, G.A. Melkov. Magnetization oscillations and waves. CRC Press, N.Y. (1996). 455 p.
[32] R.W. Damon, J.R. Eshbach. J. Phys. Chem. Solids **19**, *3–4*, 308 (1961).
[33] R.E. De Wames, T. Wolfram. J. Appl. Phys. **41**, *3*, 987 (1970).
[34] Yu.V. Gulyaev, A.S. Bugaev, P.E. Zilberman, I.A. Ignatiev, A.G. Konovalov, A.V. Lugovskoy, A.M. Mednikov, B.P. Nam, E.I. Nikolaev. JETP Lett. **30** (600), (1979). (in Russian).
[35] Y.V. Gulyaev, P.E. Zilberman, A.V. Lugovskoy. Phys. Solid State **23**, *4*, 1136, (1981). (in Russian).
[36] M.E. Seleznev, Y.V. Nikulin, Y.V. Khivintsev, S.L. Vysotsky, A.V. Kozhevnikov, V.K. Sakharov, G.M. Dudko, E.S. Pavlov, Y.A. Filimonov. Izvestiya VUZ. Applied Nonlinear Dynamics **30**, *5*, 617 (2022).
[37] M.V. Vinogradova, O.V. Rudenko, A.P. Sukhorukov. Theory of Waves. Fourth ed. Lenand, M. (2019). (in Russian).
[38] T. Wolfram, R.E. De Wames. Phys. Rev. B **1**, *11*, 4358 (1970).
[39] G.T. Kazakov, A.G. Sukharev, Yu.A. Filimonov. Phys. Solid State **32**, *12*, 3571 (1990). (in Russian).
[40] J.A. Reissland. The Physics of Phonons. John Wiley & Sons, Ltd (1973).

Translated by Ego Translating